Triple ionisation of HCl *via* states with a 2p core hole

J.H.D. Eland[1] and R. Feifel[2*]

[1]*Department of Chemistry, Physical and Theoretical Chemistry Laboratory, Oxford University, South Parks Road, Oxford OX1 3QZ, United Kingdom*
[2]*Department of Physics, University of Gothenburg, Origovägen 6B, SE-412 96 Gothenburg, Sweden*

*corresponding author: raimund.feifel@physics.gu.se

Abstract

The triple ionisation of HCl by double Auger decay and related processes has been studied using a multi-particle coincidence technique combined with synchrotron radiation. Four contributing processes are identified, direct double Auger, two indirect double Auger decay pathways and single Auger decay from core-valence doubly ionised intermediate states. One indirect Auger process involves autoionisation from superexcited states of Cl^+. Double Auger decay from HCl^+ ($2p^{-1}$, ^2P_J), which makes up 11±2% of total Auger decay, is estimated to be 40% direct, 15% indirect *via* atomic Cl^{+*} and 45% indirect *via* molecular intermediate doubly ionized states. The vertical triple ionisation energy of HCl is determined as 73.8±0.5 eV. Molecular field effects are found to affect the direct double Auger process as well as normal single Auger decay. Comparison between spectra of the HCl and DCl isotopomers indicates that electronic decay is faster in all the processes than molecular dissociation.

Introduction

Double ionisation of HCl by the Auger effect after creation of a hole in the 2p shell ($L_{23}VV$ Auger) has been thoroughly studied both experimentally and theoretically [1-5], as has the related single ionisation by resonant Auger from the 2p core excited pre-edge resonances [6-9]. Triple ionisation of this molecule has hardly been studied at all, and is the subject of this paper, but triple ionisation of HBr has been explored in detail [15]. As expected on the analogical basis that HCl is a perturbed form of atomic Ar, some observed processes are similar to those found by the same technique in triple ionisation of that atom [10, 11], but new features and pathways are introduced by the lower symmetry and by the possibility of nuclear motion.

The states of HCl^+ created by $2p^{-1}$ ionisation are almost atomic $^2P_{3/2}$ and $^2P_{1/2}$ levels with a spin-orbit splitting of 1.66 eV [1]. The molecular field produces a further splitting of the $^2P_{3/2}$ term by about 0.08 eV into $^2\Pi_{3/2}$ and $^2\Sigma_{1/2}$ states [1]; the $^2P_{1/2}$ level is reclassified as $^2\Pi_{1/2}$ in the molecular symmetry. The spectra of HCl^{++} created by single Auger emission from these states are calculated to be slightly different [2-5], the biggest difference being between the decay characteristics of the two molecular states arising from $^2P_{3/2}$. The Auger spectra are interpreted as spectra of the intact molecule, the assumption being that the lifetime of the 2p hole state (Γ = 95 meV, τ = 6.8 fs) is too short to allow significant nuclear motion. By contrast, the decay of the 2p pre-edge resonances is interpreted as involving "ultrafast dissociation" [6] of the neutral excited states followed by atomic Auger transitions in the liberated Cl atom [7-9]. This fast dissociative process is believed to carry 60% of the total decay intensity, while 40% of molecular Auger decay remains, giving a broad continuous electron spectrum underlying the resolved atomic part.

There is no known stable or metastable state of HCl^{3+}, so the process of triple ionisation is always dissociative overall. Nevertheless, because the lifetime of the inner-shell hole is so short, we expect that in direct double Auger decay, dissociation will happen mainly after formation of a nascent molecular HCl^{3+} species. We shall see in this work that this expectation is fulfilled in most of the observed decay pathways. The double Auger effect can be direct, but can also involve cascade processes through intermediate doubly ionised states, which may dissociate en route. At higher photon energies, triple ionisation can also occur with intermediate formation of a core-valence (CV) doubly ionised state. The time sequence of ionisation and dissociation events in the indirect pathways is not immediately predictable and is a major question addressed by the present experiments.

Experimental methods

Experiments were carried out at the storage ring synchrotron radiation source BESSY II of the Helmholtz Zentrum, Berlin, using beamline U49/2 PGM-2 when the ring was operated in single-bunch mode. As described more fully in the context of a laboratory light source [12], ionisation occurs where the wavelength-selected light intersects an effusive beam of target gas in the strong, inhomogeneous field of a conical permanent magnet. This magnetic field guides virtually all electrons, irrespective of their emission angle or energy into the field of a long (here ca 2.2 m) solenoid, whose field lines they follow to a distant multichannel plate (MCP) detector. The arrival times of the electrons are registered relative to the pulses of light from the storage ring by a multi-hit time-to-digital converter and are stored on a local computer. Because the flight times of low-energy electrons to the detector are longer than the interval of 800.5 ns between light pulses, specific strategies must generally be adopted to identify the pulses on which ionisation actually occurred. In all the experiments reported here the desired events include emission of a fast Auger electron with a flight time less than 800 ns, so no ambiguity arises. Nevertheless, in some experiments on DCl we used a synchronous chopper [18] to extend the inter-pulse period to 12 μs, so gaining even greater clarity and reducing noise in the spectra. The electron count rate was always kept sufficiently low such that no accidental false coincidences from multiple events on a single pulse need be considered. Calibration of the time of flight (TOF) to energy conversion was by examination of the Auger and photoelectron spectra of Xe before and after each run on HCl or DCl. Some calibration shifts caused by the effect of the gases on contact potentials were noted and compensated. The electron energy resolution measured on standard samples for single electrons was about 2%, but for multi-electron processes such as triple ionisation the final resolution depends on the electron energy distribution and must be estimated in each case for the distribution concerned.

Both the HCl and DCl samples were commercial products of stated 98 % purity. Both were allowed to flow into the apparatus for some time before measurements were started in order to condition the spectrometer surfaces. Before runs on DCl the apparatus was conditioned using D_2O until the mass spectrum showed better than 95 % isotopic purity.

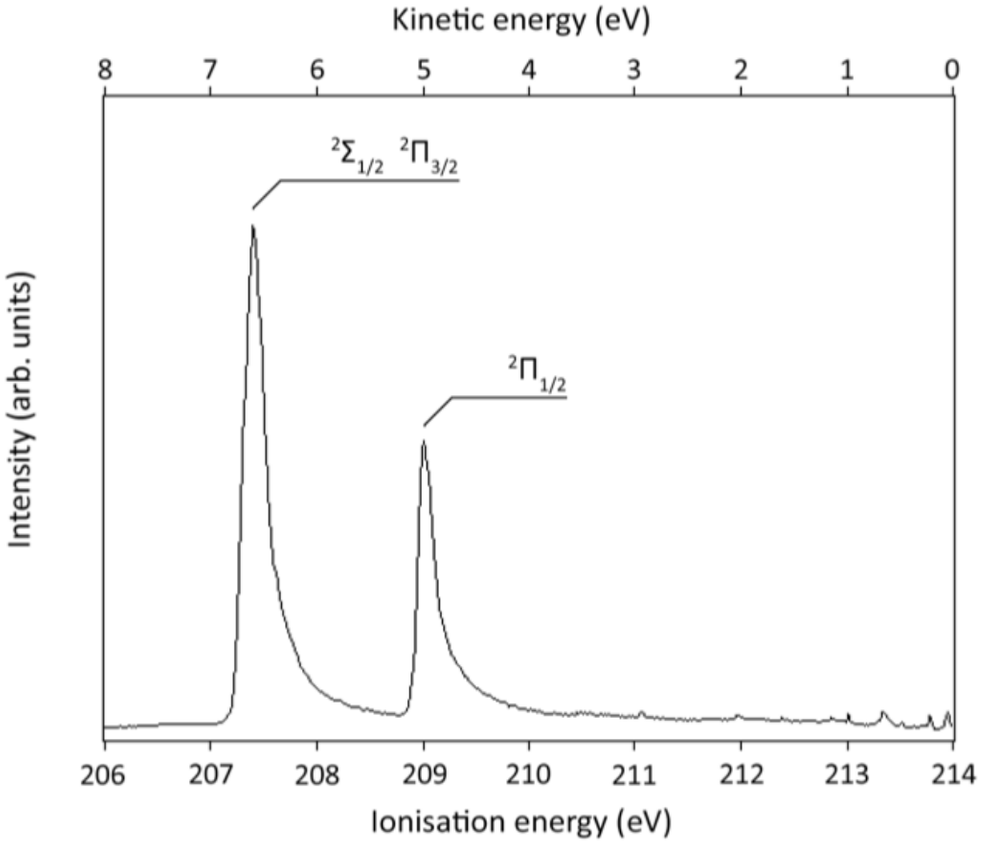

Figure 1. Low energy electrons from HCl at 214 eV photon energy showing the $^2P_{3/2}$ (molecular notation: $^2\Sigma_{1/2}$, $^2\Pi_{3/2}$) and $^2P_{1/2}$ ($^2\Pi_{1/2}$) photolines with some low-energy tailing due to PCI. Some of the small peaks at high ionisation energy are artefacts; others are real low energy autoionisation lines.

Results

Spectrum of the core holes

Fig. 1 shows a spectrum of the 2p core-ionised states of HCl^+ formed at 214 eV photon energy. Some line distortion by post-collision interaction (PCI) is present, affecting the higher energy state more than the lower one. The $^2P_{3/2}$ (molecular notation: $^2\Sigma_{1/2}$, $^2\Pi_{3/2}$) peak is wider (0.22 eV FWHM) than the $^2P_{1/2}$ ($^2\Pi_{1/2}$) peak (0.20 eV) as in previous work [1] as a result of the molecular field splitting. No vibrational structure is apparent despite the wide vibrational spacing expected (0.37 eV in HCl), which could easily be resolved. We note that we cannot disentangle the different contributions to the line shape and width. The photoelectron peaks are found at 207.45±0.05 and 209.07±.05 eV, in good agreement with the reported Rydberg series limits of 207.32 and 208.96 eV [13]. At the lowest electron energies in Fig. 1 (highest apparent ionisation energies) there are weak, sharp peaks; these arise from atomic autoionizations in dissociative Auger decays and are discussed below.

Triple ionization by double Auger decay

As two electrons are emitted in double Auger decay, the distribution of energy between them in forming triply ionized final states constitutes a spectrum in itself. Because this distribution is diagnostic of the Auger decay pathways, which affect the

final triply-ionised state spectrum, it is expedient to examine it first. In fact, we can extract a distribution of Auger electrons leading to formation of any selected energy range within the manifold of final triply ionized states, from either one of the two initial photolines. As an example, the spectrum of electrons emitted as pairs in double Auger decay from the $^2P_{3/2}$ core-hole states to triply ionised states in the energy range 70 to 80 eV is given in Fig. 2.

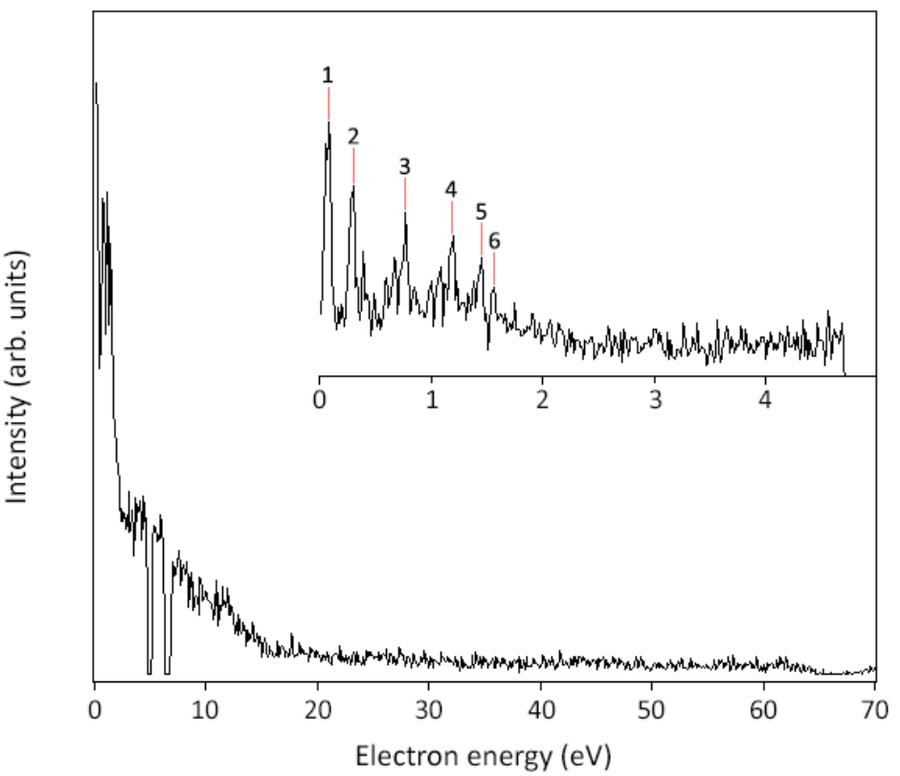

Figure 2. Low energy half of the spectrum of Auger electrons from the $^2P_{3/2}$ core hole, which contribute to triple ionization in the range 70 to 80 eV (cf. Fig. 3). The expanded spectrum shows the first 5 eV only, where the background appears different because of an increase in pixel size to allow the peaks to be resolved. Two gaps around 6 and 7 eV are at the energies of the photo lines.

The full spectrum (lower curve) has a nearly flat section from about 16 eV up to half the maximum available energy of 130 eV; we interpret this smooth part of the distribution as coming from a *direct* double Auger process. (Because of energy conservation, the spectrum from 65 eV to 130 eV would be a mirror image of the part from 0 to 65 eV, apart from the effect of instrumental resolution). At lower energy there is considerably higher intensity, rising over the range from about 15 eV down to zero, and topped by sharp peaks which can be seen more clearly in the expanded spectrum. These sharp peaks (Table 1) must be atomic autoionisations, which could in principle be either from excited Cl^{2+*} to Cl^{3+} or from Cl^{+*} to Cl^{2+}. Because the lowest asymptotic limit for $H + Cl^{3+}$ is at 81.1 eV, and the triply ionised states to which the "resonant" peaks decay are almost entirely below that energy, the final products must in fact be $H^+ + Cl^{2+}$, with lowest asymptote at 54.8 eV. Further analysis shows that the

peaks belong to Rydberg series converging on the ^2D_J levels of Cl^{2+} with limits 2.238 and 2.246 eV above $Cl^{2+}(^4S)$, as indicated in Table 1.

The unresolved part of the distribution underneath the sharp atomic lines and below 16 eV is attributed to indirect double Auger decay involving molecular rather than atomic species, where available energy is partitioned partly into translational energy of the fragments.

If the flat part of the overall Auger electron distribution extends to zero energy with no change in amplitude it will constitute about 40% of the total decay at the photon energy of 214 eV; we attribute this to the direct double Auger process. But because even direct two-electron processes have tendency towards unequal energy sharing, this is probably an underestimate. The atomic autoionisation lines then make up 15% and the remaining 45% intensity with one low and one high energy electron must be attributed to molecular cascade double Auger, probably involving partial dissociation of an intermediate. We emphasize that the percentages stated are only rough estimates and that is in practice very challenging to separate the two contributions to the double Auger decay. In fact, how to properly parameterize the energy sharing distributions of two electron emission processes is currently the matter of in-depth investigations (see e.g. Ref. [19] and refs. therein).

We can now extract triple ionisation spectra of HCl from double Auger decays of HCl^+ selected in coincidence with the $^2P_{3/2}$ photoelectron line, following the direct and indirect pathways. Triple ionisation spectra from double Auger decay of HCl^+ selected in coincidence with the $^2P_{3/2}$ photoelectron line at a photon energy of 214 eV are shown in Fig. 3.

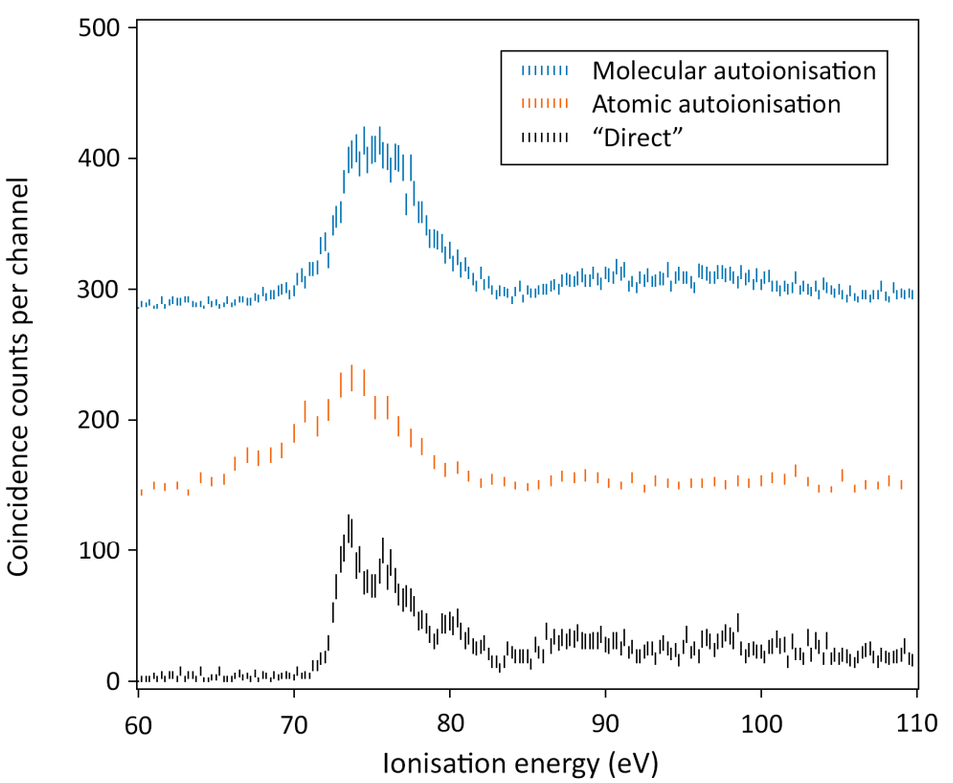

Figure 3. Triple ionisation of HCl by double Auger decay from the $^2P_{3/2}$ hole state, created by ionization at 214 eV photon energy. Lowest spectrum: "Direct" double Auger decay, taking electrons with energies greater than 16 eV. Middle spectrum: Indirect double Auger decay via the atomic autoionisation lines below 0.3 eV. Upper spectrum: Indirect double Auger decay via assumed molecular intermediates emitting electrons of 3-16 eV energy. The bars for the data points reflect 2σ error bars.

The bottom spectrum in Fig. 3 is derived from the direct part of the pair distribution, i.e. taking Auger electrons with more than 16 eV energy; it has a sharp onset near 72 eV, peaks at 73.8 and 76 eV, a shoulder at 77.5 eV and a further peak 80.2 eV. From the energies and spacing of these bands compared with the spacing of 3.7 eV between $X^2\Pi$ and $A^2\Sigma$ in the photoelectron spectrum [14] we could attribute three of them in simple molecular terms to ionisations from the outermost π and σ orbitals, involving three transitions expressed as losses from individual orbitals, π^{-3} (73.8 eV), $\pi^{-2}\sigma^{-1}$ (77.5 eV) and $\pi^{-1}\sigma^{-2}$ (80.8 eV). This attribution does not explain the peak at 76 eV and ignores both spin and spin-orbit splitting effects. The π^1 configuration (from π^{-3}), for instance, generates 2 spin-orbit states $^2\Pi_{3/2}$ and $^2\Pi_{1/2}$ with an expected splitting of about 0.2 eV which would not be noticed. But $\pi^2\sigma^1$ from $\pi^{-2}\sigma^{-1}$ generates 4 distinct electronic states $^{2,4}\Sigma^-$, $^2\Delta$, $^2\Sigma^+$ whose spacings are not so easily predictable. The lowest state, to which we assign the peak at 73.8 eV, is certainly expected to be the $^2\Pi$ state with dominant configuration $[Ne]3s\sigma^2 3p\pi$. This attribution to molecular states is in line with the idea that the direct DA process involves the least possible delay between creation of the inner-shell hole and formation of the triply ionised products. An alternative attribution involving partial dissociation to atoms is also discussed below.

The middle spectrum in Fig. 3 is selected from double Auger decays which include emission on the two sharp lines (at 0.03 eV and 0.26 eV, lines 1 and 2 of the inset) shown in Fig. 2. The most intense peak is at the same energy as in the direct process, but the spectrum extends to lower triple ionisation energies, with a possible step or onset at about 66 eV. Because the autoionising lines are sharp, the process generating them must involve at least partial dissociation and an additional delay from the lifetime of the intermediate state. Spectra from the individual atomic lines in both HCl and DCl are discussed later in the paper in connection with the mechanism of these decays (Fig. 8).

The spectrum in the upper panel of Fig. 3 shows the triple ionization spectrum generated from the part of the Auger electron distribution attributed to indirect *molecular* processes. It also extends to lower ionization energy than the direct spectrum, but less far than the spectrum from atomic autoionisation. There is a gradual low energy tail with no distinct onset.

To examine whether the molecular field in core-ionized HCl affects the double Auger spectrum, we have also extracted final state HCl^{3+} spectra in coincidence with different parts of the $^2P_{3/2}$ photoline, at least partially isolating the two overlapping molecular components. The resulting HCl^{3+} spectra are shown in Fig. 4.

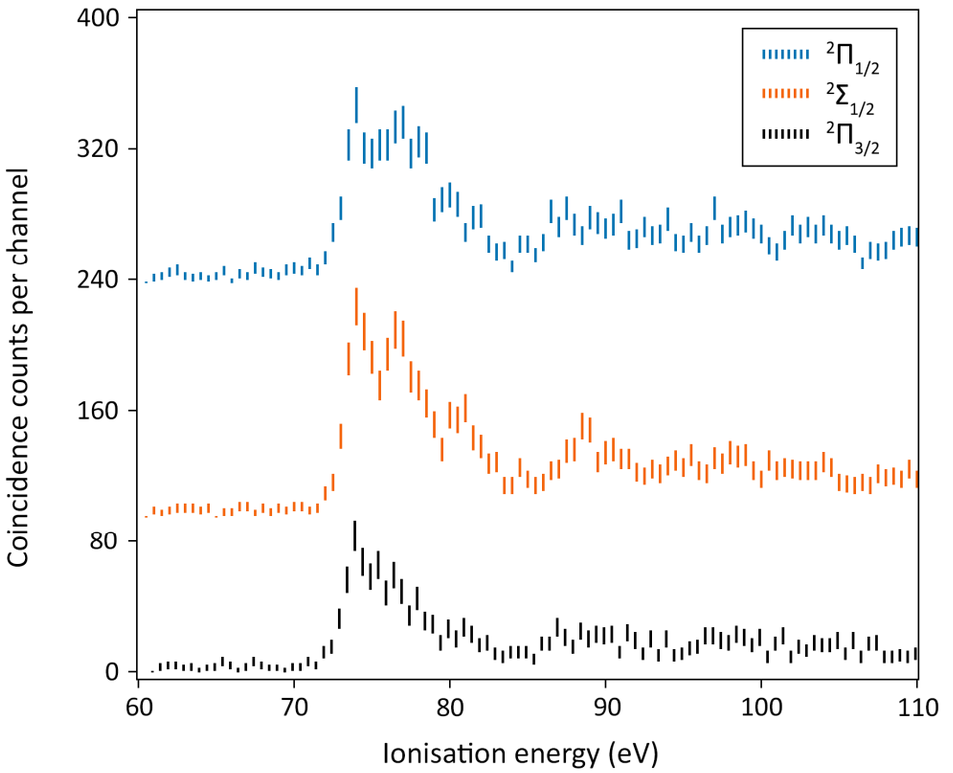

Figure 4. Spectra of HCl^{3+} formed by direct double Auger decay from distinct parts of the ^2P hole manifold differentiated in the molecular field. The direct process was selected by restricting the second Auger electron to energies above 16 eV in all events. The $^2\Pi$ and $^2\Sigma$ components of $^2P_{3/2}$ were (partially) isolated by taking only the lowest binding energy part of the $^2P_{3/2}$ peak for $^2\Pi_{3/2}$, and the shoulder and tail on the high energy side for $^2\Sigma_{1/2}$. The bars for the data points reflect 2σ error bars.

When electron pairs of all energies are included, there is no perceptible difference in the final-state spectra. But when direct double Auger is selected by requiring the slower Auger electron to have more than 16 eV energy (as in the bottom spectrum of Fig. 3), notable differences appear between the final state spectra. Fig. 4 demonstrates distinct differences between final state spectra from the different parts of the photolines affected by the molecular field. They confirm in particular that the two molecular components of the $^2P_{3/2}$ hole state have indeed been selected differentially.

In all of these spectra, resolution is limited by the energies of the Auger electrons. In the spectra of Fig. 3 and Fig. 4 the best instrumental resolution is estimated as about 2 eV, comparable with the width of the narrowest peaks observed.

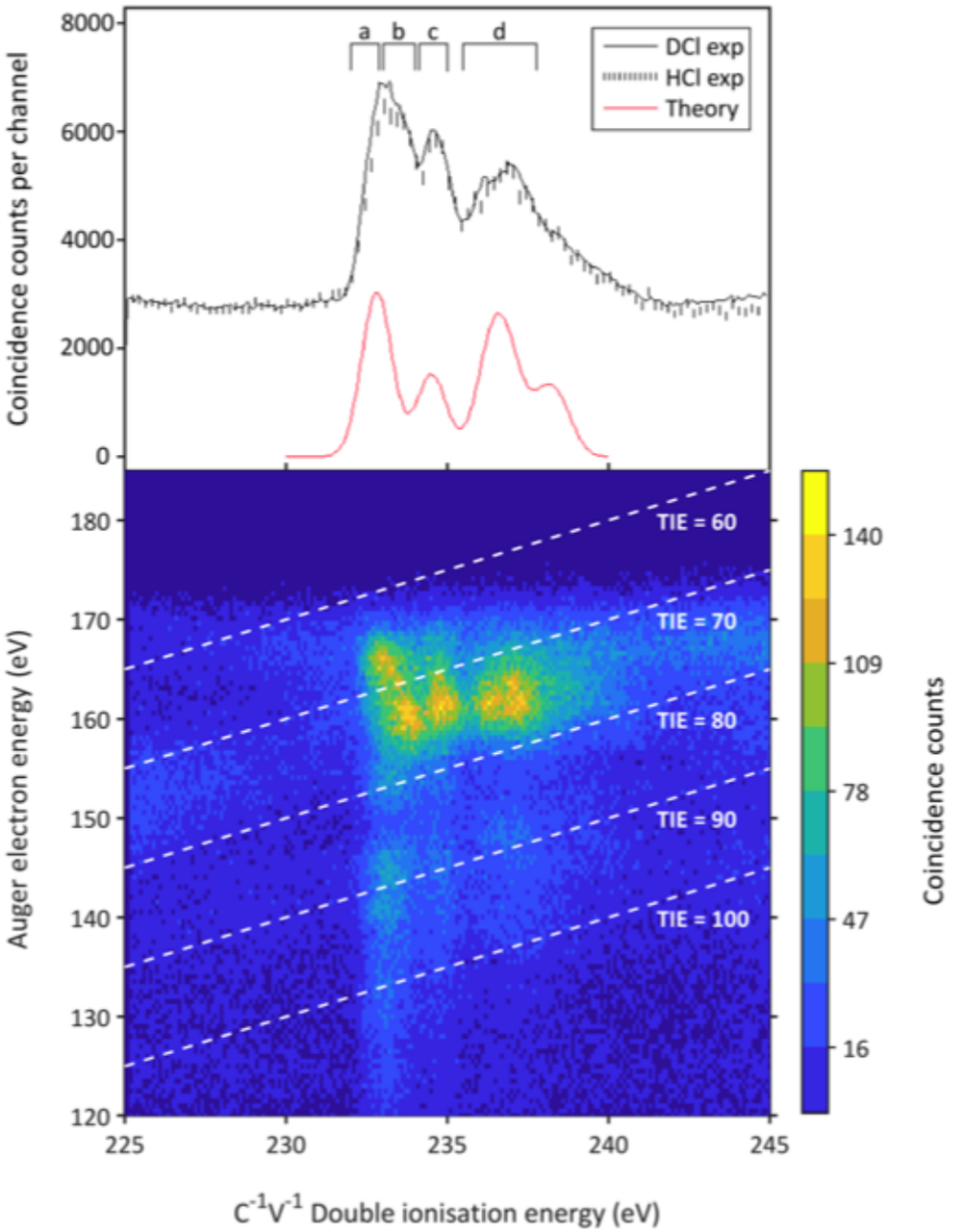

Figure 5. Upper panel: Core-valence double ionisation spectrum of HCl (error bars) and DCl (full line) taken at 260 eV photon energy, with a model spectrum derived from the HeI photoelectron spectrum as explained in the text. The scale of coincidence counts refers to the DCl data, which have the better statistics in this case. The counts for HCl can be deduced from the lengths of the 2σ error bars. Note that the base lines for the measured spectra are offset (+ 2000 in the case of DCl). Lower panel: Coincidence map showing the formation and Auger decay of core-valence doubly ionised states in DCl at hν = 260 eV. Points of equal triple ionisation energy are represented by the white, dashed, sloped lines. The map for HCl is indistinguishable from this one.

Core–valence ionisation and its consequences

The upper panel of Fig. 5 shows $2p^{-1}\ V^{-1}$ core-valence spectra of HCl and DCl taken at 260 eV photon energy. They are indistinguishable in form and contain two unequal peaks at around 234 eV, separated by about 1.6 eV, which we interpret as mainly $2p^{-1}3p\pi^{-1}$ ionisation duplicated 2:1 by spin-orbit splitting in the $2p^5$ core. The doublet is followed by a broader band where the spin-orbit splitting is not resolved, which we attribute mainly to $2p^{-1}3p\sigma^{-1}$ ionization by analogy with the valence photoelectron spectrum [14]. A full interpretation of the CV spectrum is expected to be much more complex, because as many as 10 states arise from the different allowable combinations of orbital and spin angular momenta. Fortunately, the singlet-triplet and other splittings in these states are likely to be small as in other CV spectra. This simple interpretation is used to build a model spectrum drawn below the experimental ones; it consists simply of the valence photoelectron spectrum [14] duplicated in 2:1 intensity ratio at 1.66 eV separation and folded with a Gaussian to represent the apparatus function. But the apparent simplicity of the CV spectrum is not matched by its decay behaviour, which is revealed in the coincidence map, lower panel of Fig. 5, of intensity as a function of the slow electron pair energy (E2 + E3, forming the CV state) and E1, the Auger electron energy released in the CV states' decay to triply charged products.

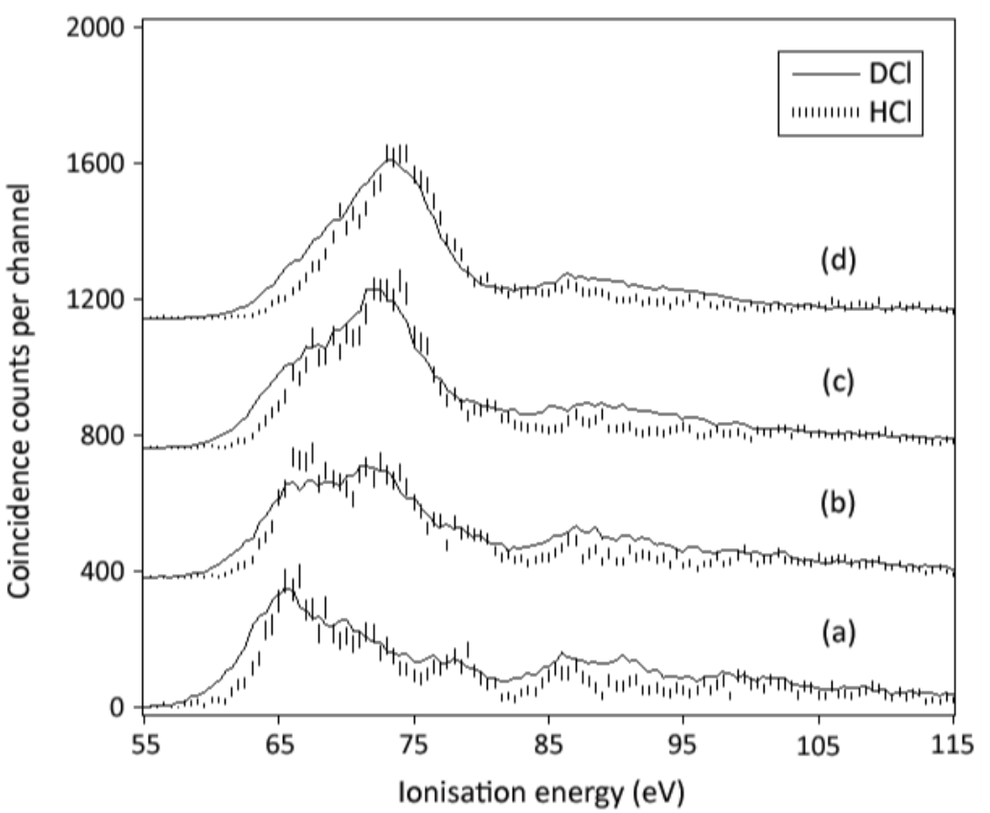

Figure 6. Final state spectra of HCl^{3+} (error bars) and DCl^{3+} (full lines) from Auger decay of four different sections of the core-valence spectra, as marked in the upper panel of Fig. 5. The apparent shift of the DCl spectra to lower ionisation energies is not thought to be real, but is attributed to a difference in resolution and calibration at the times of the different experiments.

Fig. 6 shows four spectra of triply ionised $[HCl]^{3+}$ and $[DCl]^{3+}$ in coincidence with selected electron pairs corresponding to components of the CV bands as marked in the upper panel of Fig. 5. The zones a-d chosen reflect our best attempt to emphasize differential selection of the different major components, with the experimental resolution in mind. Section (a) shows the final-state spectra from the very lowest energy CV component, attributed to combinations of the $^2P_{3/2}$ $^2\Pi_{3/2}$ core hole with a valence $3p\pi^{-1}$ ionisation, which formally produce 8 distinct states. Spectra in (b) arise from the $^2P_{3/2}$ $^2\Sigma_{1/2}$ core hole and a $3p\pi^{-1}$ ionisation (2 states), while those in (c) are thought to involve a $^2P_{1/2}$ $^2\Pi_{1/2}$ core hole. The topmost spectra, (d), come from high-energy CV states involving $2p^{-1}$ ionisation and $5\sigma^{-1}$ ionisation from the valence shell. All these spectra extend at least partly to energies below the vertical triple ionisation energy of 73.8 eV estimated from the spectrum of direct double Auger (lowest spectrum in Fig. 3). Triple ionisation spectra (a), from the lowest energy CV state, have their first and strongest peaks at about 67 eV, followed by a series of weaker peaks at intervals of about 6 eV. This spectrum is similar in the spacing of its components to the spectrum of single Auger decay from the $^2P_{3/2}$ $^2\Pi_{3/2}$ core hole as calculated by Fink et al. [5]. In their spectrum a difference between the spectra from HCl and DCl is detected. On energy grounds we know that the state at 67 eV binding energy must represent $Cl^{2+} + H^+$ partially separated products (threshold 54.8 eV) because $Cl^{3+} + H$, with threshold at 81.1 eV, is excluded. Dissociation can occur only in the core-valence state or in the triply ionised state, as there is no other intermediate. In decay from the $2p^{-1}\sigma^{-1}$ CV initial states (d) the main peak of intensity is at a final binding energy of about 74 eV and there are fewer higher energy peaks.

Discussion and further analysis

The behaviour of HCl in triple ionisation by double Auger decay from the $2p^{-1}$ core hole states is very similar to the behaviour of HBr in similar circumstances [15]. To avoid needless repetition of the points already made by Penent et al. in their paper [15], we concentrate here mainly on observations peculiar to our study of double Auger processes in HCl, and on the information from core-valence states, which were not included in the HBr work [15].

Direct triple ionisation by DA

In direct triple ionisation by double Auger decay, the spectrum of HCl^{3+} has a much sharper onset than in the case of HBr [15], and there is a marked effect of the molecular field in the core-ionised state. It is notable in Fig. 4 that double Auger decay from the $^2\Sigma_{1/2}$ component of $^2P_{3/2}$ populates the HCl^{3+} state attributed to $\pi^{-2}\sigma^{-1}$ ionization more strongly than does decay from the $^2\Pi_{3/2}$ component. It also populates a higher excited state at 89 eV, which is not apparent in the overall spectrum.

If triply charged "molecules" formed in the lowest vertically populated state(s) of HCl^{3+} at energies near 73.9 eV decay to $H^+ + Cl^{2+}$, the only energetically possible products, we can calculate the kinetic energy release for each atomic state of Cl^{2+}. For ground state (^4S) of Cl^{2+} the kinetic energy must be 73.9 – 54.8 = 19.1 eV, for Cl^{2+} (^2D) it would be 16.9 eV and for Cl^{2+} (^2P) it would be 15.4 eV. But if the potential energy surface is assumed to be Coulombic, these energies must correspond to the internuclear distances at the time of triple ionisation, which can be compared with the bond distance in the initial state. If the products are in the ground state, they appear to have come from a state of $H^+ + Cl^{2+}$ with an internuclear distance of 1.5 Å, while for the first two excited products the distances are 1.7 and 1.9 Å respectively. The bond

length in neutral HCl is 1.275 Å and in the core-ionised states, which have bound potential energy surfaces, it is calculated to lie between 1.284 and 1.288 Å [16]. The fit is clearly best for dissociation to ground state products, which correlate to just one single molecular symmetry ($^4\Sigma$). It is possible that direct double Auger decay populates this state directly, although it belongs to the first excited configuration ($Ne5\sigma2\pi^2$) in the molecular symmetry. The excited products $H^+ + Cl^{2+}(^2D)$ correlate formally to three molecular states ($^2\Sigma$, $^2\Pi$, $^2\Delta$), and if the initial triply-charged state is essentially atomic already and dissociates on a single curve, we should expect a peak in the spectrum at 73.9 +2.2 = 76.1 eV; this is exactly the position of the second clear peak in the spectrum (Fig. 3, lowest spectrum). There are hints of a higher peak, which could represent formation of $H^+ + Cl^{2+}(^2P)$, but this is rather unclear. At higher energies there are weaker and broader peaks which probably show the formation of $H^{\cdot} + Cl^{3+}$, which is possible at energies above 81.1 eV. For such products the potential energy surface is not remotely Coulombic unless charge exchange takes place, so there may be any kinetic energy release from zero upwards. Overall, we conclude that direct double Auger decay indeed populates essentially *atomic* triply ionized products.

Indirect triple ionization via autoionizing states of superexcited Cl^+

The existence of this pathway was clearly demonstrated in the related case of HBr [15], where the autoionizing states could be assigned to Rydberg series converging on the resolved spin-orbit levels of $Br^{2+}(^2D)$. In HCl we do not resolve the spin-orbit splitting in Cl^{2+} (8 meV), but find that most of the lines belong to a similar series with an integer quantum defect (Table 1), as also found by Penent et al. for HBr [15]. If the defect is near zero the active electron must be in a d- or f- orbital, but if the defect is about unity, a p-orbital would be likely. One strong line with n^*=5.2 does not fit into the main series.

From the energies of the sharp lines and the identification of the series as converging to $Cl^{2+}(^2D)$, we know that the final products of these decays are $H^+ + Cl^{2+}(^4S)$. The measured energies of the final triply ionized state then leave only one quantity not directly measured, namely the kinetic energy released in the dissociation. Neglecting dissociation in the original hole state, this KE can arise in the doubly ionized intermediate state, in the triply ionized products or from a combination of both. It can be determined from the final state energy simply by subtracting the thermodynamically known dissociation limit (54.8 eV). Spectra of the final states reached *via* the four strongest sharp lines are shown in Fig. 7, where differences between spectra from the different lines can be seen. Because it was thought that the characteristics of this pathway might be affected by isotopic substitution, equivalent measurements were made for DCl, and are also shown, but there is no significant detectable difference between the two isotopologues.

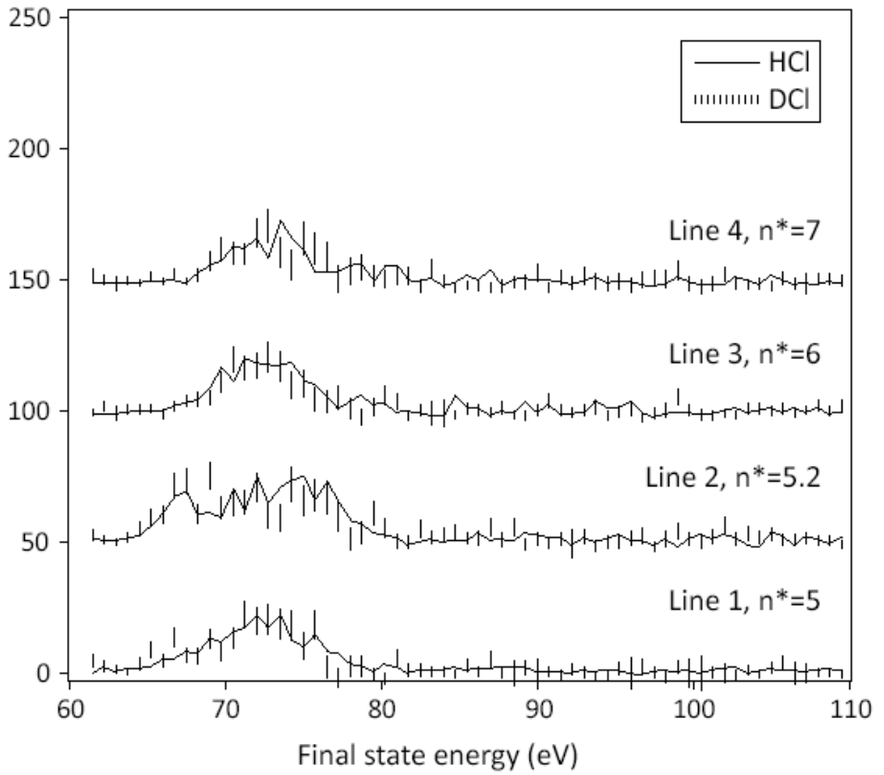

Figure 7. Binding energy spectra of the final states of $[HCl]^{3+}$ formed by double Auger decay from all the $2p^{-1}$ (^2P) hole states and producing sharp atomic autoionisation lines of Cl^{+}*. The continuous lines are data for HCl and error bars show results for DCl.

The formation of these final state spectra can be modelled using some simple assumptions, with the lifetime of the intermediate state as one principal parameter. We suppose that the intermediate starts out as an HCl^{3+} ion core with an initial 1.3 Å bond distance, with one external Rydberg electron. If the proton or deuteron was already charged in this intermediate state it would immediately start to separate from the Cl^{2+} ion core, eventually pass beyond the Rydberg electron radius (hydrogenic estimate n^2a_0/Z) and then accelerate further, first on a dicationic repulsive Coulomb potential e^2/r_{12} until autoionisation, then afterwards on the tricationic potential $2e^2/r_{12}$. In contrast, if the hydrogen atom in the initial molecular Rydberg state is uncharged, the potential energy surface would be almost flat and located near the appearance energy of Cl^{3+}, 81 eV. In this scenario no Coulombic energy release would occur until after autoionisation.

If the potential energy is defined at each internuclear distance in pure Coulombic repulsion, the time taken to reach each distance can be calculated analytically; the formula has been given in convenient form by Last et al. [17]. The final state spectrum should depend mainly on the autoionising state's lifetime. For instance, if the lifetime is much longer than the dissociation time, and initial acceleration within the Rydberg electron orbit can be neglected (H initially uncharged), the spectrum should have a peak for ground state products ($H^+ + Cl^{3+}(^4S)$) at 66 eV, corresponding to decay entirely on the $H^+ + Cl^{+}$* potential and autoionization at asymptotic distance. For any shorter lifetime there will be less intensity at 66 eV (54.8 +14.4/1.3) and more intensity towards the highest limit, 77

eV (54.8 + 28.8/1.3) where the whole decay is on the triply-charged potential surface. It is striking that almost all the experimental intensity lies between these two limits. From overall exponential decay of the superexcited Cl^{+}* population we must expect decays over a range of individual lifetimes and therefore final energies, as observed. Some limits on the lifetimes are set by the observed linewidths and the uncertainty principle. The narrowest line, line 2, is 20 meV wide, of which the majority is instrumental width. Thus, its lifetime towards autoionisation must be longer than 32 fs. The width of line 1 is greater, approximately 30 meV ($\tau \geq 22$ fs) while the higher lines are too weak for accurate width estimation. In general, Rydberg lifetimes towards autoionisation are expected to rise with increasing n*.

To check the reasonableness of this model, we need estimates of dissociation times to compare with the lifetimes. A typical total kinetic energy release is 20 eV (ionisation energy 74.8 eV). In the molecular Rydberg state, the potential energy as a function of H—Cl distance may not be flat, but cannot be quite as steep as tricationic because of the extra electron. As a compromise, let us assume it is dicationic, e^2/r, as opposed to the final tricationic surface $2e^2/r$. For a total kinetic energy release of 20 eV the crossover of the two surfaces, where autoionisation is most likely to occur, is at 1.6 Å and kinetic energies in the two steps are 2.1 eV and 17.9 eV respectively. The time for the bond distance to increase in the first step from 1.3 to 1.6 Å is roughly 2 fs for H^+ or 3 fs for D^+, both of which are much shorter than the Rydberg state lifetimes. Thus, we consider this model of dissociation preceding autoionisation to be reasonable, though obviously subject to correction by fuller theoretical calculations. We also note that the likely Rydberg electron radii are longer than the estimated crossover distance. On the basis of the hydrogenic orbital radius and equating n with n* the radius is 4.4 Å for n*=5 and goes up to 11.3 Å for n*=8.

Other points to note from Fig. 7 are that only line 2, which does not belong to the same Rydberg series as the others, gives a significantly different final state profile, and that no difference in pattern between H and D is seen.

Triple ionisation via the core-valence states

It is at first very puzzling that Auger decay from the lowest energy CV state, which we identify as having a $^2P_{3/2}(\Pi_{3/2})$ core and a $^2\Pi$ valence vacancy and is therefore the most likely of all the CV states to have a bound potential energy surface (though perhaps with a different equilibrium bond length), gives triple ionization to dissociated products at the lowest final binding energies. The main peak in spectrum (a) of Fig. 6 is at 65 eV and corresponds to an energy release of 65-54.8 = 10.2 eV. For dissociation on a triply charged repulsive Coulomb potential this would require dissociation from an initial bond distance of 2.9 Å. Decays from the higher energy CV states (spectra b to d in Fig. 6) have peaks near to the vertical triple ionisation energy of 73.8, and so appear to decay from the original bond distance of 1.3 Å. The CV states' lifetimes towards Auger decay might seem unlikely to be very different from that of the normal Cl 2p hole of 6.8 fs, which would be about sufficient to extend the bond distance to 2.9 Å on a doubly charged surface. The differences in Fig. 6 would then be inexplicable. But here comparison with the decay of the isoelectronic CV states of Ar^{2+}, examined in detail by Huttula et al. [11], is helpful. In that case both theoretical calculations and experimental peak widths showed that the lifetimes of CV states could be significantly longer (up to 65 fs) or shorter (down to 1.4 fs) compared with the bare hole lifetime of 5.5 fs. The lowest energy CV states tended to have the longest lifetimes. If the lowest energy CV states in HCl^{2+} also have longer lifetimes than higher states, and if all the states have similar dissociative (possibly Coulombic)

potential surfaces, the differences in Fig. 6 between decay from the different CV states are explained. The low energy CV states with long decay lifetimes will be able to expand before Auger decay despite their relatively bound character, while higher CV states decay on short lifetimes and so fail to extend their bond distances before Auger decay despite involving a σ-orbital valence vacancy and supposedly having more dissociative character. The mid-energy CV states exhibit intermediate, or mixed behaviour for which we must probably seek more profound theoretical explanations.

Particularly in decay from the lowest HCl^{2+} CV state, we also see formation of higher $[HCl]^{3+}$ final states, most clearly apparent in Fig. 6. Very similar formation of highly excited states of Ar^{3+} from CV state decay is reported by Huttula et al. [11] and attributed to higher configurations of the triply ionised atom.

Conclusions

Using a state-of-the-art multi-particle coincidence technique combined with synchrotron radiation from a storage ring we have explored the triple ionisation of HCl, which is seen to proceed by four main mechanisms and multiple individual pathways, mostly indirect. Only the pathway described as direct double Auger decay gives a spectrum attributable to a vertical transition at the ground state geometry, from which we derive a triple ionisation energy of 73.8±0.5 eV. All other pathways exhibit lower triple ionisation onsets, extending in the case of intermediate core-valence ionization almost to the lowest thermodynamic dissociation limit at 54.8 eV. From interpretation of the spectra we model these processes as dissociations on doubly-charged potential surfaces, followed by autoionisations to the final products. The triple ionisation energy and the energies of the core-valence states are in reasonable agreement with the results of calculations by the MCSCF method with an aug-cc-pVTZ basis set [20]. The full patterns of observed energies, spectra and relative intensities of different mechanisms call for more elaborate and extensive high-level calculations, which are not available to us at this time.

Acknowledgements

This work has been financially supported by the Swedish Research Council (VR) and the Knut and Alice Wallenberg Foundation, Sweden. We thank the Helmholtz Zentrum Berlin for the allocation of synchrotron radiation beam time and the staff of BESSY-II for particularly smooth running of the storage ring during the single-bunch runtime. The research leading to these results has received financial support from the European Community's Seventh Framework Programme (FP7/2007-2013) under grant agreement no. 312284 and from the Helmholtz Zentrum Berlin. We thank R.J. Squibb for his assistance in formatting the figures and manuscript.

References

[1] H. Aksela, E. Kukk, S. Aksela, O-P. Sairanen, A Kivimäki, E. Nommiste, A. Ausmees, S.J. Osborne and S. Svensson, *J. Phys. B: At. Mol. Opt. Phys*. **28** (1995) 4259.

[2] O.M. Kvalheim, *Chem. Phys. Lett*., **98** (1983) 457.

[3] E.Z. Chelkowska and F.P. Larkins, *Atomic Data Nucl. Data Tables*, **49** (1991) 121.

[4] A.G. Kochur, S.A. Novikov and V.L. Sukhorukov, Chem. Phys. Lett., **222** (1994) 411.

[5] R.H. Fink, M. Kivilompolo, H. Aksela and S. Aksela., *Phys. Rev. A*, **58** (1998) 1988.

[6] O. Björneholm, O. Nilsson, A. Sandell, B. Hernnäs and N. Martensson, *Phys. Rev. Lett.*, **68** (1992) 1892.
[7] H. Aksela, S. Aksela, M. Ala-Korpela, O.-P. Sairanen, M. Hotokka, G.M. Bancroft, K.H. Tan and J. Tulkki, *Phys. Rev. A*, **41** (1990) 6000.
[8] A. Menzel, B. Langer, J. Viefhaus, S.B. Whitfield and U. Becker, *Chem. Phys. Lett.*, **258** (1996) 265.
[9] R. Feifel, F. Burmeister, P. Salek, M.N. Piancastelli, M. Bässler, S.L. Sorensen, C. Miron, H. Wang, I. Hjelte, O. Björneholm, A. Naves de Brito, F.Kh. Gel'mukhanov, H. Ågren and S. Svensson, *Phys. Rev. Lett.*, **85** (2000) 3133.
[10] Y. Hikosaka, P. Lablanquie, F. Penent, T. Kaneyasu, E. Shigemasa, R. Feifel, J.H.D. Eland and K. Ito, *Phys. Rev. Lett.*, **102** (2009) 013002.
[11] S.-M. Huttula, P. Lablanquie, L. Andric, J. Paladoux, M. Huttula, S. Sheinerman, E. Shigemasa, Y. Hikosaka, K. Ito and F. Penent, *Phys. Rev. Lett.*, **110** (2013) 113002.
[12] J.H.D. Eland, *J. Electron Spectrosc. Related Phenom*., **144-147** (2005) 1145.
[13] K. Ninomiya, E. Ishiguro, S. Iwata, A. Mikuni and T. Sasaki, *J. Phys. B: At. Mol. Opt. Phys.*, **14** (1981) 1777.
[14] S. Svensson, L. Karlsson, P. Baltzer, B. Wannberg, U. Gelius and M.Y. Adam, *J. Chem. Phys.*, **89** (1988) 7193.
[15] F. Penent, P. Lablanquie, J. Paladoux, L. Andric, G. Gamblin, Y. Hikosaka, K. Ito and S. Carniato, *Phys. Rev. Lett*., **106** (2011) 103002.
[16] K. Ellingsen, T. Saue, H. Aksela and O. Gropen, *Phys. Rev. A*, **55** (1997) 2743.
[17] I. Last, I. Schek and J. Jortner, *J. Chem. Phys*., 107 (1997) 6685.
[18] S. Plogmaker, P. Linusson, J.H.D. Eland, N. Baker, E.M.J. Johansson, H. Rensmo, R. Feifel and H. Siegbahn, *Rev. Sci. Instrum*., **83** (2012) 013115.
[19] J. Andersson, S. Zagarodskikh, A. Hult Roos, O. Talaee, R.J. Squibb, D. Koulentianos, M. Wallner, V. Zhaunerchyk, R. Singh, J.H.D. Eland, J.M. Rost, and R. Feifel, Scientific Reports (submitted).
[20] D. Koulentianos, personal communication.

Table 1 Autoionising lines of Cl^+ going to $Cl^{2+}(^4S)$ (Fig. 2)

Line	Energy	n*
	eV ±.05	(converging to $Cl^{2+}\ ^2D_{5/2}$)
1	.03	4.96
2	.24	5.22
3	.72	5.98
4	1.14	7.05
5	1.39	8.05
6	1.53	8.85

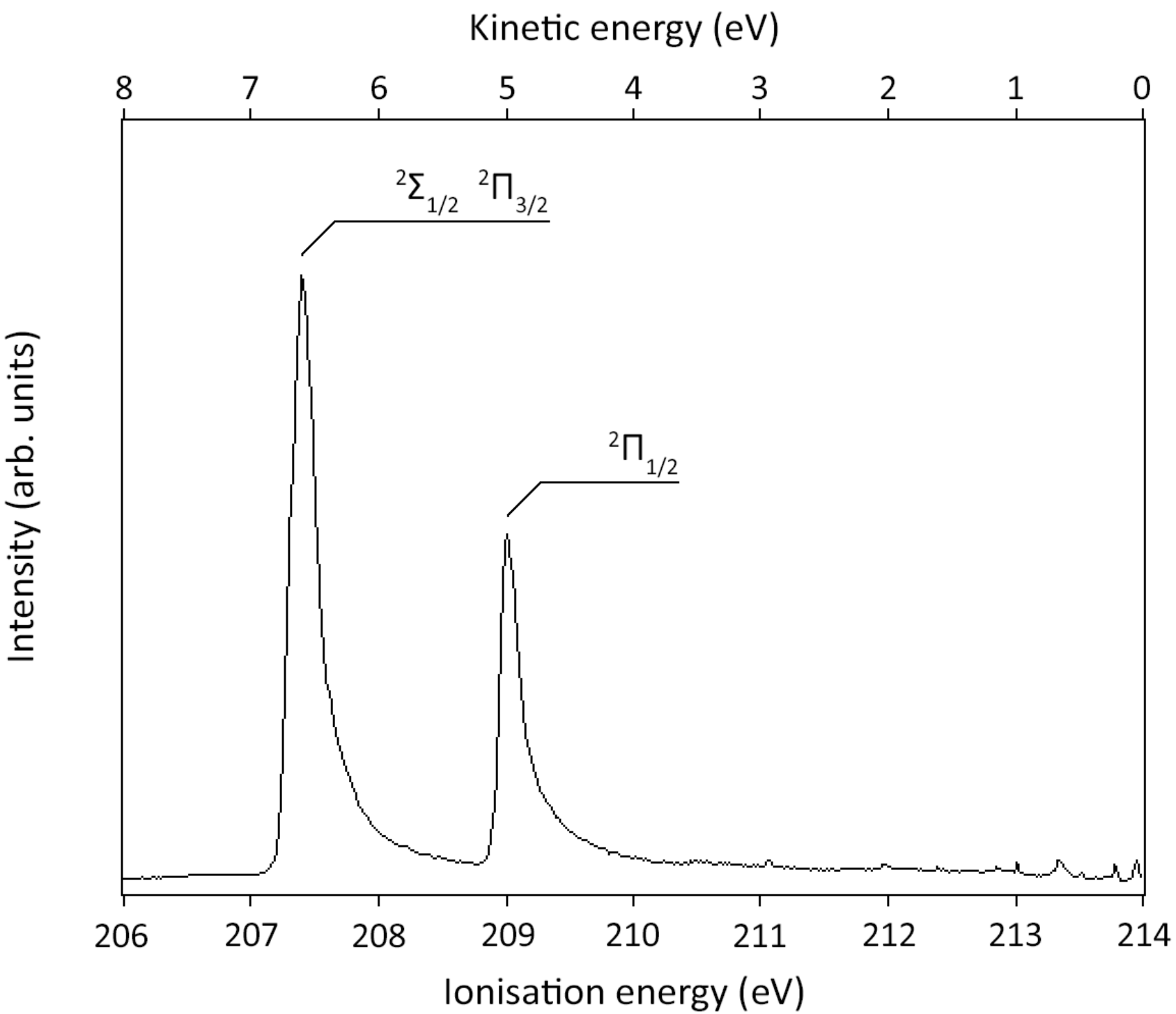
Kinetic energy (eV)
8
7
6
5
4
3
2
1
0
$^2\Sigma_{1/2}$ $^2\Pi_{3/2}$
$^2\Pi_{1/2}$
Intensity (arb. units)
206
207
208
209
210
211
212
213
214
Ionisation energy (eV)

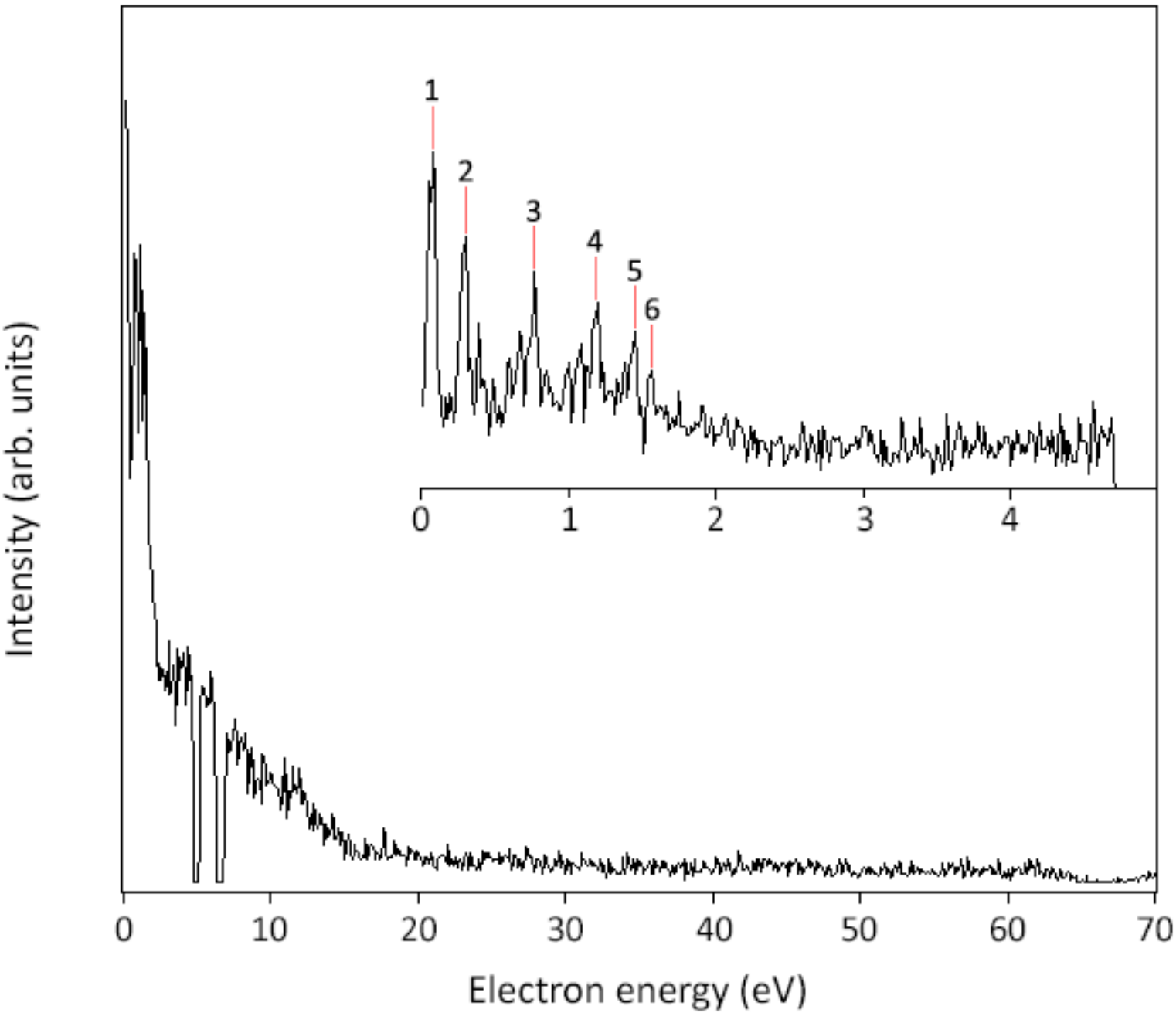
Intensity (arb. units)
1
2
3
4
5
6
0
1
2
3
4
0
10
20
30
40
50
60
70
Electron energy (eV)

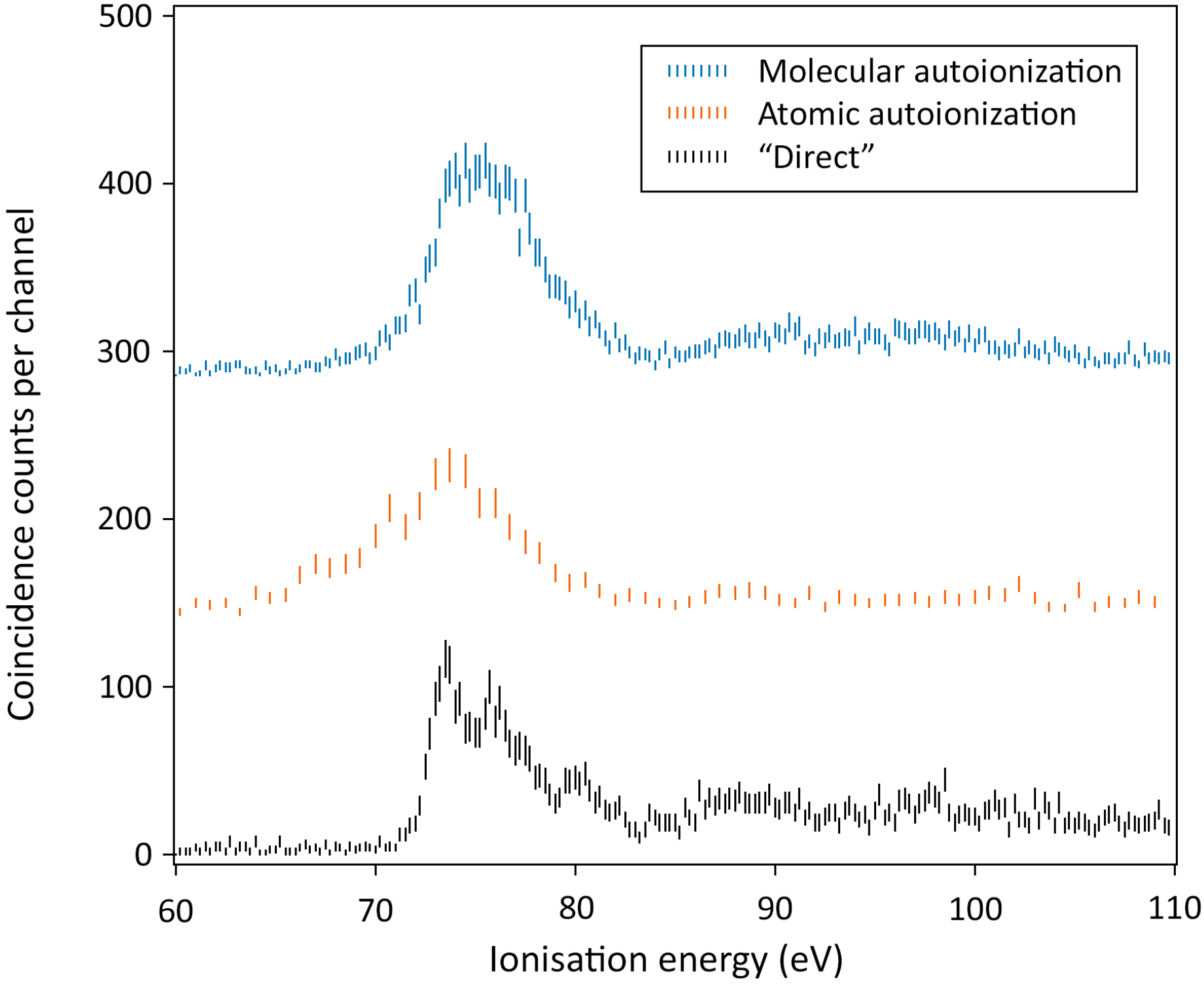
Molecular autoionization
Atomic autoionization
“Direct”
Coincidence counts per channel
0
100
200
300
400
500
60
70
80
90
100
110
Ionisation energy (eV)

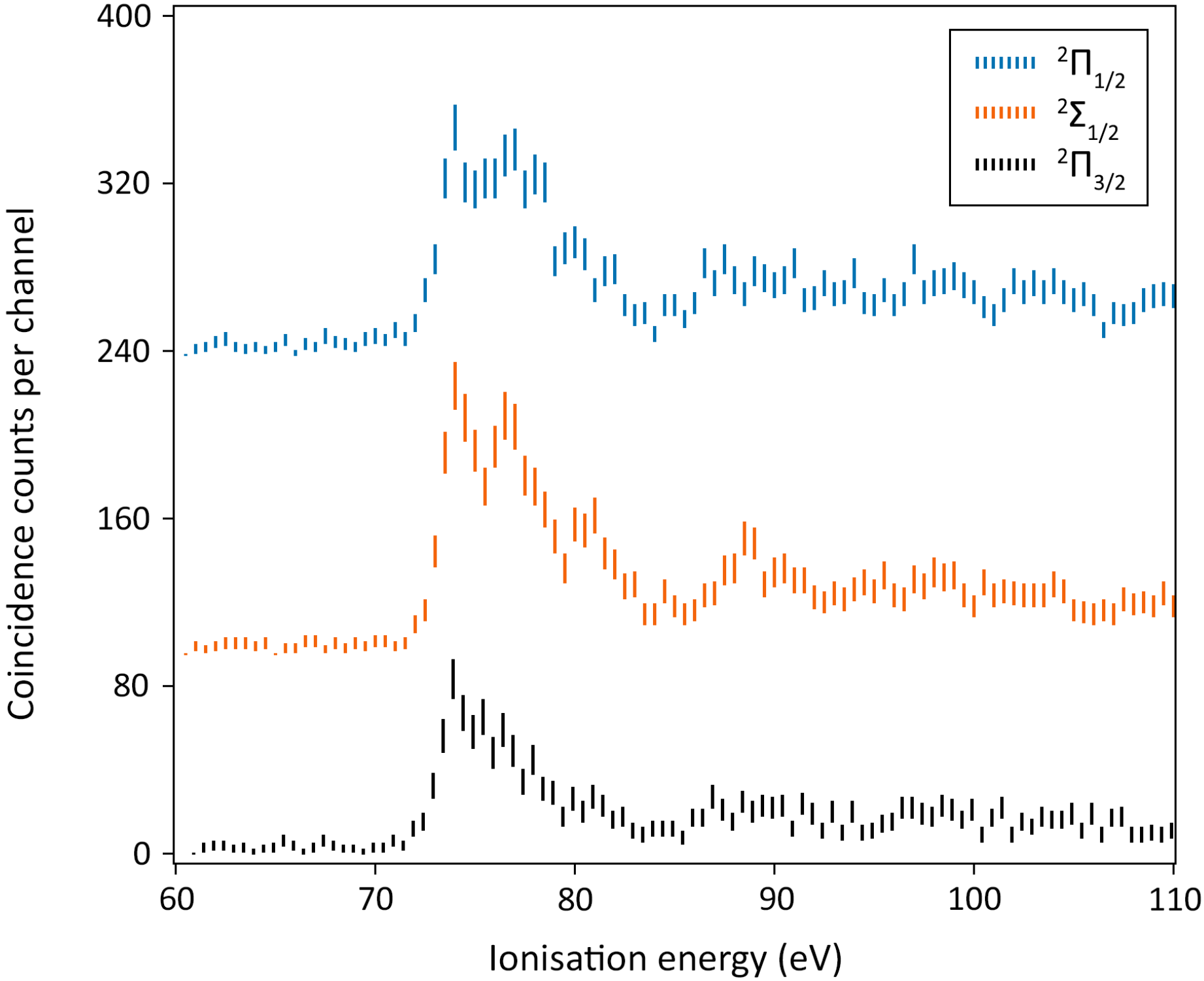
400
320
240
160
80
0
Coincidence counts per channel
60
70
80
90
100
110
Ionisation energy (eV)
$^2\Pi_{1/2}$
$^2\Sigma_{1/2}$
$^2\Pi_{3/2}$

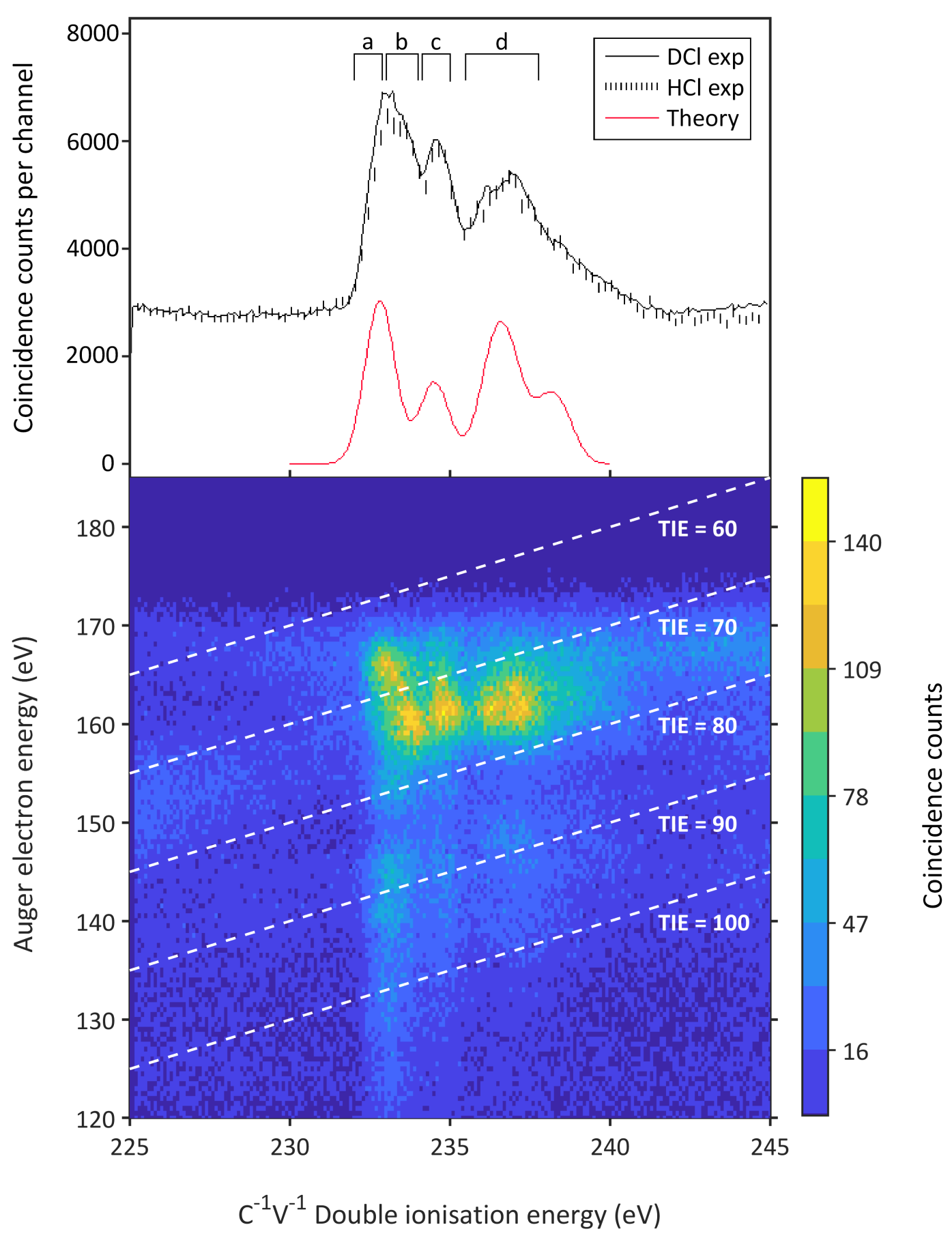
Coincidence counts per channel
8000
6000
4000
2000
0
a
b
c
d
DCl exp
HCl exp
Theory
Auger electron energy (eV)
180
170
160
150
140
130
120
TIE = 60
TIE = 70
TIE = 80
TIE = 90
TIE = 100
225
230
235
240
245
C-1V-1 Double ionisation energy (eV)
Coincidence counts
140
109
78
47
16

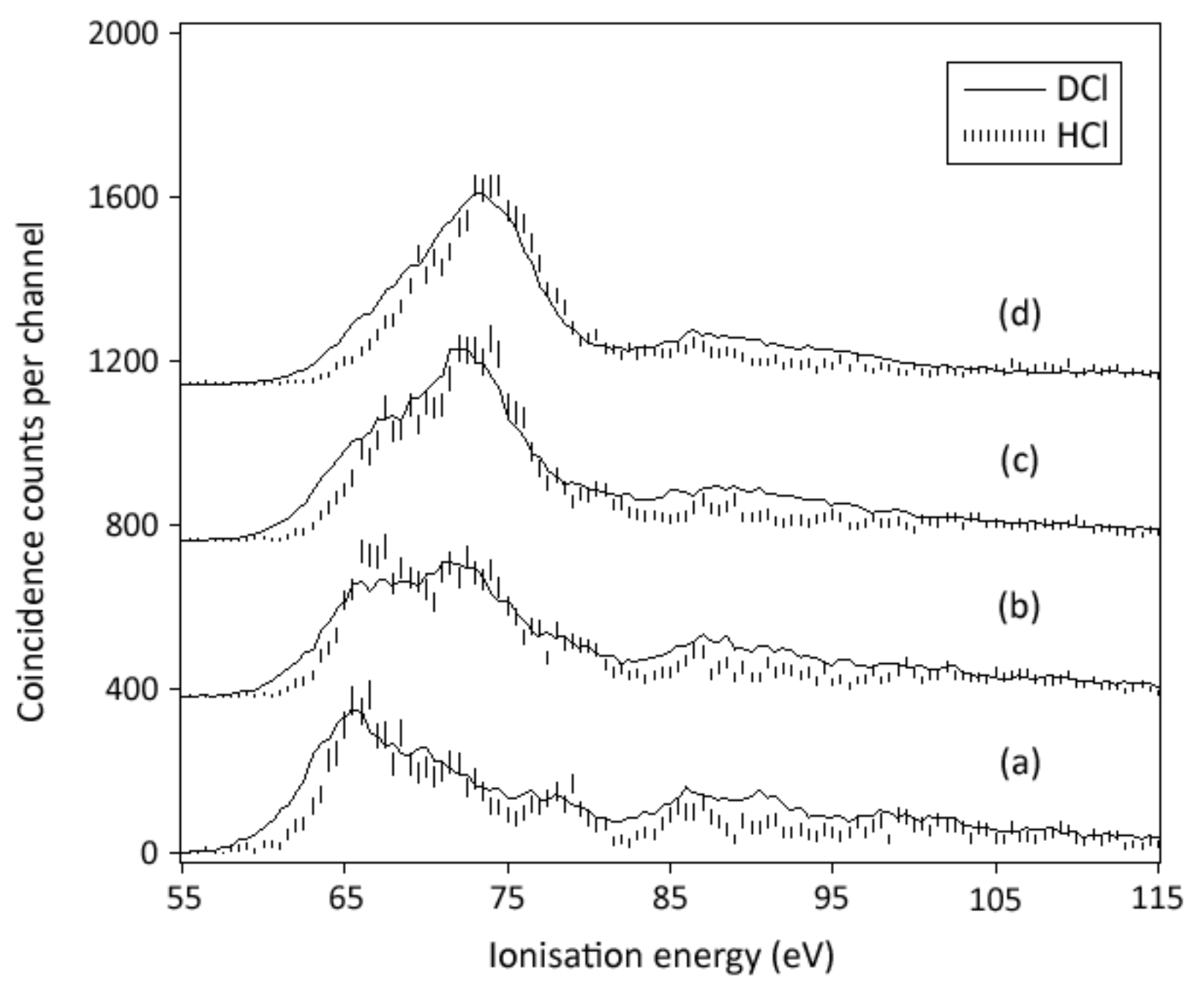
2000
1600
1200
800
400
0
Coincidence counts per channel
DCl
HCl
(d)
(c)
(b)
(a)
55
65
75
85
95
105
115
Ionisation energy (eV)

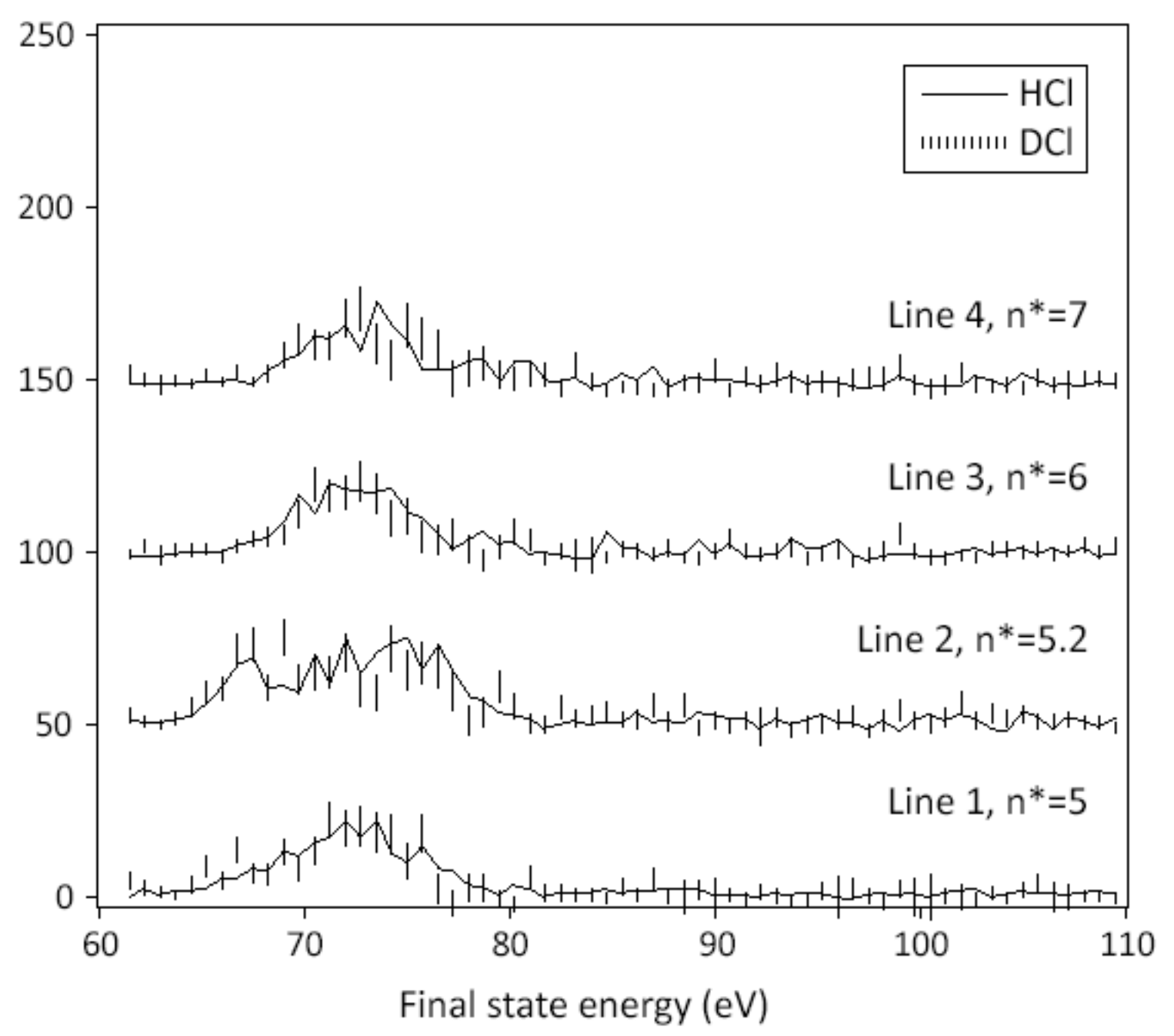
HCl
DCl
Line 4, n*=7
Line 3, n*=6
Line 2, n*=5.2
Line 1, n*=5
250
200
150
100
50
0
60
70
80
90
100
110
Final state energy (eV)